5280–5290 *Nucleic Acids Research, 2006, Vol. 34, No. 18* *Published online 29 September 2006*
doi:10.1093/nar/gkl519

Hypothesis: bacterial clamp loader ATPase activation through DNA-dependent repositioning of the catalytic base and of a *trans*-acting catalytic threonine

Andrew F. Neuwald

Cold Spring Harbor Laboratory, 1 Bungtown Road, PO Box 100, Cold Spring Harbor, NY 11724, USA

Received June 2, 2006; Revised July 5, 2006; Accepted July 6, 2006

ABSTRACT

The prokaryotic DNA polymerase III clamp loader complex loads the β clamp onto DNA to link the replication complex to DNA during processive synthesis and unloads it again once synthesis is complete. This minimal complex consists of one δ, one δ′ and three γ subunits, all of which possess an AAA+ module—though only the γ subunit exhibits ATPase activity. Here clues to underlying clamp loader mechanisms are obtained through Bayesian inference of various categories of selective constraints imposed on the γ and δ′ subunits. It is proposed that a conserved histidine is ionized via electron transfer involving structurally adjacent residues within the sensor 1 region of γ's AAA+ module. The resultant positive charge on this histidine inhibits ATPase activity by drawing the negatively charged catalytic base away from the active site. It is also proposed that this arrangement is disrupted upon interaction of DNA with basic residues in γ implicated previously in DNA binding, regarding which a lysine that is near the sensor 1 region and that is highly conserved both in bacterial and in eukaryotic clamp loader ATPases appears to play a critical role. γ ATPases also appear to utilize a *trans*-acting threonine that is donated by helix 6 of an adjacent γ or δ′ subunit and that assists in the activation of a water molecule for nucleophilic attack on the γ phosphorous atom of ATP. As eukaryotic and archaeal clamp loaders lack most of these key residues, it appears that eubacteria utilize a fundamentally different mechanism for clamp loader activation than do these other organisms.

THE CLAMP LOADER COMPLEX

The tracking of prokaryotic DNA polymerase III along the replication fork during DNA synthesis requires a topological link to DNA. This is provided by the β subunit, which functions as a sliding clamp [reviewed in (1,2)] to keep the catalytic α subunit on the DNA for tens of thousands of base pairs or more without dissociating (3,4). Two β subunits associate to form a stable homodimeric ring (5) that thus must be opened for loading onto DNA before DNA synthesis and for unloading once DNA replication is completed. This loading and unloading reaction is catalyzed by the γ clamp loader (6–8) [reviewed in (9)], the minimal complex of which consists of one copy each of the δ and δ′ subunits and three copies of the γ subunit (designated γ_B, γ_C and γ_D) (10,11). All three types of subunits possess an AAA+ module (11,12). AAA+ modules typically function in the assembly and disassembly of protein complexes [reviewed by (13)] and are characterized by an N-terminal P loop ATP-binding domain (14) (domain I) followed (C-terminally) by a helical bundle domain (domain II). Only the γ AAA+ module exhibits ATPase activity; δ and δ′ do not. All three subunits also contain a C-terminal domain (domain III). Although this minimal γ complex has been extensively used for *in vitro* analyses, *in vivo* two τ subunits replace two of the γ subunits, which are encoded by the same gene as the τ subunit, but—owing to a translational frameshift—lack an additional C-terminal extension that plays a critical role in binding of the clamp loader to core polymerase (15). These two forms of the clamp loader complex may be treated as identical for our purposes here.

The eukaryotic and archaeal clamp loader complexes, termed replication factor C (RFC), similarly harbor AAA+ modules with attached C-terminal domains and are thought to be functionally analogous to the bacterial γ complex [reviewed in (16)]. Unlike the γ complex, however, the eukaryotic complex contains five distinct subunits: RFC-A (corresponding to δ), RFC-B, RFC-C and RFC-D (corresponding to γ_B, γ_C and γ_D, respectively), and RFC-E (corresponding to δ′), whereas the archaeal clamp loader complex typically contains only two types of subunits: RFCL (corresponding to δ) and RFCS (corresponding to both γ and δ′).

Numerous structural studies provide insights into bacterial clamp loaders. These include crystal structures (i) of isolated γ and δ′ subunits (17,18), (ii) of ATP, ADP and nucleotide

Tel: +1 516 367 6802; Fax: +1 516 367 8461; Email: neuwald@cshl.org

free forms of the minimal γ complex (11,19) and (iii) of a complex of the δ subunit bound to the β clamp (20). These studies reveal that the five clamp loader subunits mutually interact via their third C-terminal domains. These domains are arranged in the order δ-γ_B-γ_C-γ_D-δ′ to form a circular collar from which the AAA+ modules hang (11). Crystal structures are also available for the yeast RFC clamp loader bound to an ATP analog and the clamp (21) and for two archaeal RFC homotrimeric subcomplexes each of which consists of three RFCS subunits and where four of the six RFCS subunits are bound to ADP (22).

Mutational and biochemical studies have helped in interpreting these structural data and vice versa, resulting in a fairly detailed model (Figure 1A) for the sequence of events mediated by the γ complex. For example, based on the structure of the δ–β complex (20) it was proposed that, within the full γ complex, the δ subunit induces conformational changes at the β-clamp dimeric interface thereby triggering an inherent spring-loaded mechanism in the β-clamp's ring to open it. This model is supported by biochemical studies indicating that the δ subunit alone can open and remove β clamps from DNA nearly as efficiently as the γ complex itself (7) and that it does this by opening only one of the two β-clamp monomeric interfaces (23), so that the opened β ring retains its dimeric structure. Other studies reveal that ATP binding increases affinity of the γ complex for DNA (24,25) and point to several residues within γ and δ′ subunits likely involved in DNA binding (26). These studies also reveal that the γ complex uses ATP binding and hydrolysis to modulate its interaction with DNA: the ATP-bound form binds with high affinity to ordinary DNA whereas association with elongation-proficient DNA preferentially triggers ATP hydrolysis and conversion to a low-affinity state (27). Thus, upon contact with cognate DNA the clamp loader–clamp complex undergoes ATP hydrolysis resulting in closure of the clamp around DNA [for reviews see (2,9,28,29)].

STATISTICAL INFERENCE OF CLAMP LOADER FUNCTIONAL CONSTRAINTS

Previous studies raise additional questions regarding the molecular and structural details associated with the bacterial clamp loader mechanism. A critical question specifically addressed here is how association of the γ complex with DNA activates ATP hydrolysis. Although further biochemical and structural studies are required, of course, to answer this question, designing such experiments is nontrivial and requires that one first formulate feasible hypotheses through preliminary observations. One such source of observations is to apply Bayesian statistics to infer the various categories of functional constraints imposed by underlying mechanisms [(30,31) and references therein; recently reviewed in (32)]. When examined in the light of the biochemistry and

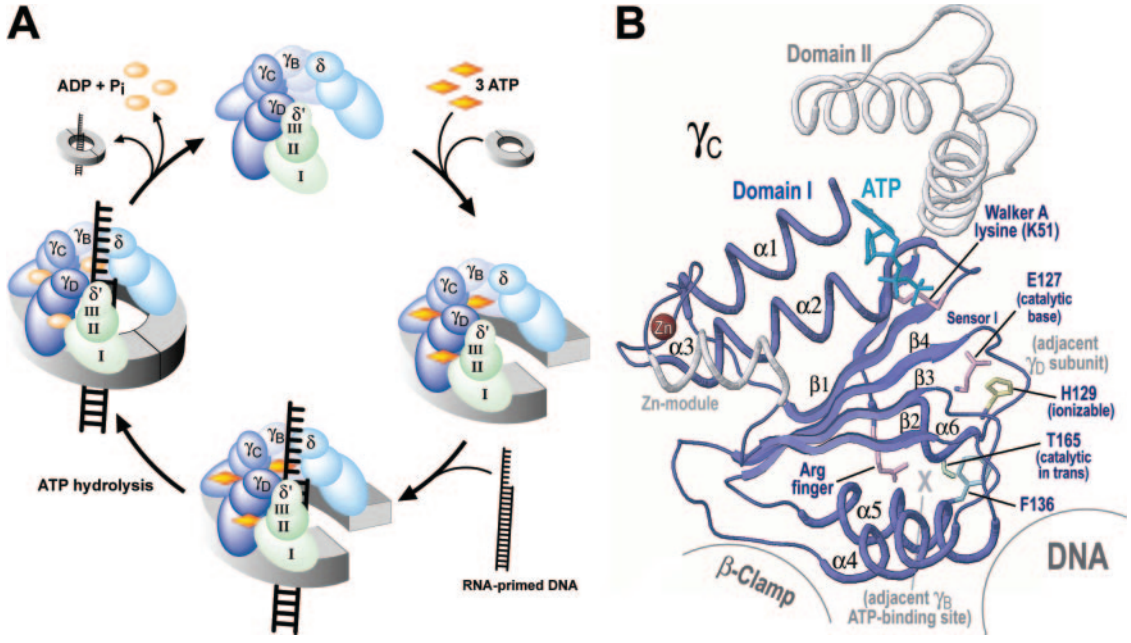

Figure 1. Relevant features of the bacterial clamp loader complex and of γ ATPase. (**A**) The sequence of events mediated by the γ clamp loader [reviewed in (53,54)]. The γ complex consists of five semicircularly arranged subunits (1 δ, 1 δ′ and 3 γ) that in the presence of ATP bind to and open the β clamp. Upon association with RNA-primed DNA this complex undergoes ATP hydrolysis to load the clamp onto DNA. Each of these subunits contains three domains (I, II and III); domains I and II correspond to an AAA+ module whereas domain III forms a collar holding the complex together. (**B**) Relevant structural regions within the AAA+ module of γ ATPase. Domain I, which is the focus of this article, is shown in blue. Also shown are three AAA+ catalytic residues (in light magenta): the Walker A lysine ($Lys51^{\gamma}$), which forms hydrogen bonds with phosphate groups of bound ATP; the putative catalytic base ($Glu127^{\gamma}$) that follows the Walker B motif and that is proposed to mediate nucleophilic attack by a water molecule on the γ phosphate of ATP; and an arginine finger ($Arg169^{\gamma}$) that is proposed to interact with and facilitate hydrolysis of ATP bound to an adjacent γ subunit. (The δ′ subunit, which contacts the ATP-binding site of the adjacent γ_D subunit, also conserves this arginine finger.) Loop regions connected to the N-terminal and C-terminal ends of helix 4 are predicted to interact with DNA and with the β clamp, respectively. The locations of adjacent γ subunits (γ_B and γ_D) relative to the central subunit (γ_C) are indicated, along with three key residues discussed in the text: His129 (yellow side-chain), Phe136 (light cyan) and Thr165 (light green). This structure corresponds to pdb code 1NJF (18). This figure was created using RasMol (55).

structures of clamp loader proteins, such constraints can provide valuable clues regarding the mechanistic roles of specific residues.

Such an analysis of the eukaryotic RFC–clamp loader complex (33) recently led to a number of hypotheses regarding its underlying mechanism, including that (i) RFC ATPases are activated upon interaction with DNA through a conformational switch where an arginine moves away from a position in which it disrupts the conformation of key catalytic residues and into the central hole of the clamp loader complex, through which DNA is thread; (ii) residues uniquely conserved within the RFC-A subunit trigger this Walker

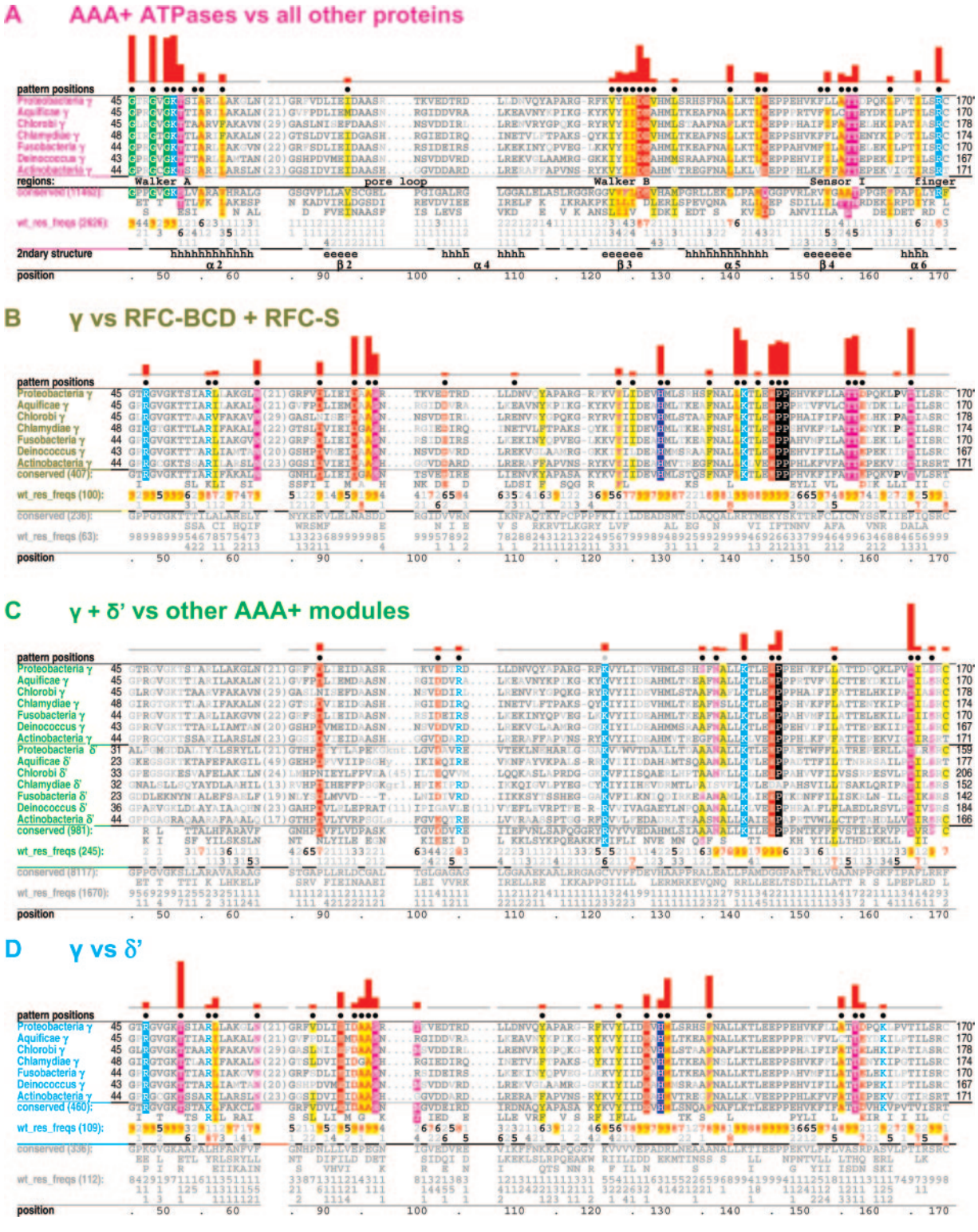

B-arginine conformational switch upon contact with DNA; (iii) the RFC-B, RFC-C and RFC-D subunits conserve residues involved in propagating this switch between adjacent RFC ATPases; and (iv) a lysine interacting with the C-terminal end of helix 4, which directly interacts with the clamp, plays a key role in clamp binding, clamp release or both [reviewed in (32)].

A similar analysis of constraints imposed on bacterial γ and δ′ subunits (shown in Figure 2) reveals critical features that strikingly diverge from those of corresponding eukaryotic RFC subunits and that suggest feasible hypotheses regarding bacterial clamp loader mechanisms. Interpreting these bacteria-specific features, however, requires that we first consider the roles of several key residues in γ that are generally characteristic of AAA+ ATPases.

DISTINGUISHING FEATURES OF AAA+ ATPASES

Functional constraints that the γ subunit shares with active AAA+ ATPases are shown in Figure 2A. AAA+ ATPases belong to the large superclass of sensor 1-like P loop NTPases, which are characterized by three conserved motifs: the Walker A and B motifs (14,34) followed by a third motif, termed sensor 1 or motif C (35). The Walker A motif (GxxxxGKT) consists of residues that bind to the phosphates of ATP. The Walker B motif consists of a string of hydrophobic residues forming a β strand followed by an acidic residue (Asp126γ) that binds to the Mg^{2+} ion coordinating with ATP. In AAA+ ATPases the sensor 1 region typically conserves an asparagine or threonine ($Thr157^{\gamma}$) that sometimes forms a hydrogen bond with the γ-phosphate of ATP and thus can sense nucleotide binding or hydrolysis (17). In other AAA+ ATPases sensor 1 residues contribute to a network of hydrogen bonds positioning a water molecule near the γ-phosphate of ATP (36,37) presumably thereby facilitating nucleophilic attack (38).

AAA+ ATPases typically also conserve a putative 'arginine finger' (39) ($Arg169^{\gamma}$) that appears to play a key role in the hydrolysis of ATP bound to an adjacent AAA+ subunit (2,11,29,40). The δ′ subunit also conserves this arginine ($Arg158^{\delta'}$), which is predicted to interact with ATP bound to the adjacent γ_D subunit. Mutational analysis of these arginines (41) indicates that they also play a structural role associated with the clamp loader's affinity both for the β clamp (the δ′ arginine) and for DNA (the γ_D and γ_C arginines).

KEY RESIDUES IN γ INTERACTING WITH THE PUTATIVE CATALYTIC BASE

Constraints distinguishing bacterial clamp loader ATPases (γ subunits) from catalytically inactive δ′ subunits (Figure 2D) are likely to conserve key residues involved in coupling DNA-dependent ATP hydrolysis to clamp loading. Indeed two conserved residues in this category ($Arg47^{\gamma}$ and $Thr52^{\gamma}$) directly bind to ATP within γ crystal structures whereas another, the glutamate ($Glu127^{\gamma}$) directly following the Walker B aspartate, plays a critical catalytic role. This glutamate is likely to serve as the catalytic base facilitating nucleophilic attack on the γ-phosphate of ATP by an activated water molecule, inasmuch as mutational and biochemical analysis indicated such a role for the equivalent residue in the ABC transporter BmrA (42). $Glu127^{\gamma}$ is structurally located next to a highly conserved histidine ($His129^{\gamma}$ in Figure 3A) that also distinguishes γ from δ′ (Figure 2D). In many γ crystal structures, $His129^{\gamma}$ appears to form a hydrogen bond with a side-chain oxygen of the proposed catalytic glutamate ($Glu127^{\gamma}$)—though whether this involves a strong –NH or a weak –CH hydrogen bond cannot be determined from the electron densities for these structures (but see below).

Eukaryotic and archaeal RFC–clamp loader ATPases lack this histidine and instead conserve an acidic residue at this position, as do many other AAA+ ATPases. This implies that, in principle, this histidine is dispensable for the clamp loading catalytic reaction. Conversely, bacterial γ subunits generally fail to conserve an arginine that appears essential to the function of the corresponding RFC–clamp loaders ($Arg84^{RFC\text{-}B}$ in Figure 3B). Within the RFC complex this

Figure 2. Statistical inference of selective constraints imposed on γ and δ′ ATPases. An alignment of domain I of γ from distinct prokaryotic taxa (as indicated in the leftmost column) is highlighted in four ways to reveal four distinct categories of constraints. Each alignment visualizes the degree to which conserved residues in the 'proteins-of-interest' have diverged from a 'reference group' of proteins and thus reveals the change in selective pressure between these two protein 'functional states' (32). Bayesian and other statistically based procedures were used to optimally align and define these two groups such that the proteins-of-interest share a strikingly conserved pattern that is strikingly nonconserved in the reference group. [Application of these procedures—which is termed CHAIN analysis (31)—involves various types of Markov chain Monte Carlo procedures (30) and modified versions of PSI-BLAST (56), as described previously (31). The alignment procedures also rely on information derived from structural alignments (57) and from close examination of available crystal structures, as described previously (58). For statistical details see (30,31) and references therein; for a recent review see (32).] Conserved patterns characteristic of the proteins-of-interest are shown directly below each alignment with corresponding residue frequencies given in integer tenths below these patterns (an '8' in integer tenths, for example, indicates that the corresponding residue occurs in 80–90% of these sequences). Directly below this [in (B–D)] the patterns and residue frequencies for the reference group are likewise shown. [Patterns and residue frequencies for the reference group in (A), which consists of all proteins, are not shown.] Selective constraints are measured in terms of the number of random trials required to obtain the residues observed in the proteins-of-interest at each position by randomly drawing from the distribution of residues in the reference group at that position. Aligned residue positions with compositions that closely resemble the reference group will thus be found to have little or no selective constraints (because, in this case, few random trials are required), while residue positions with compositions highly incompatible with the reference group will be found to have strong constraints (because many trials are required). Each alignment displays this measure both explicitly in the histogram at the top (using a quasi-logarithmic scale) and qualitatively through highlighting of aligned residues. (**A**) Constraints distinguishing AAA+ ATPases from all other proteins. (**B**) Constraints distinguishing bacterial γ subunits from corresponding eukaryotic and archaeal RFC–clamp loader subunits. This reveals the selective constraints presumably associated with aspects of γ's function that differ from eukaryotic and archaeal clamp loader functions. (**C**) Constraints distinguishing γ and δ′ subunits, both of which interact with an adjacent γ subunit's ATP-binding site, from other AAA+ modules. (**D**) Constraints distinguishing γ from δ′ subunits. Sequence identifiers are Proteobacteria (*Escherichia coli*), pdb_id=1NJFD(γ) and 1XXIJ(δ′); Aquificae (*Aquifex aeolicus*), ncbi_gi=15606894(γ) and 2983903(δ′); Chlorobi (*Chlorobium tepidum*), ncbi_gi=21674147(γ) and 21647607(δ′); Chlamydiae (*Chlamydophila caviae*), ncbi_gi =29840095(γ) and 29834617(δ′); Fusobacteria (*Fusobacterium nucleatum*), ncbi_gi=19713068(γ) and 29834617(δ′); Deinococcus (*Deinococcus radiodurans*), ncbi_gi=15807400(γ) and 29834617(δ′); Actinobacteria (*Thermobifida fusca*), ncbi_gi=72160455(γ) and 29834617(δ′).

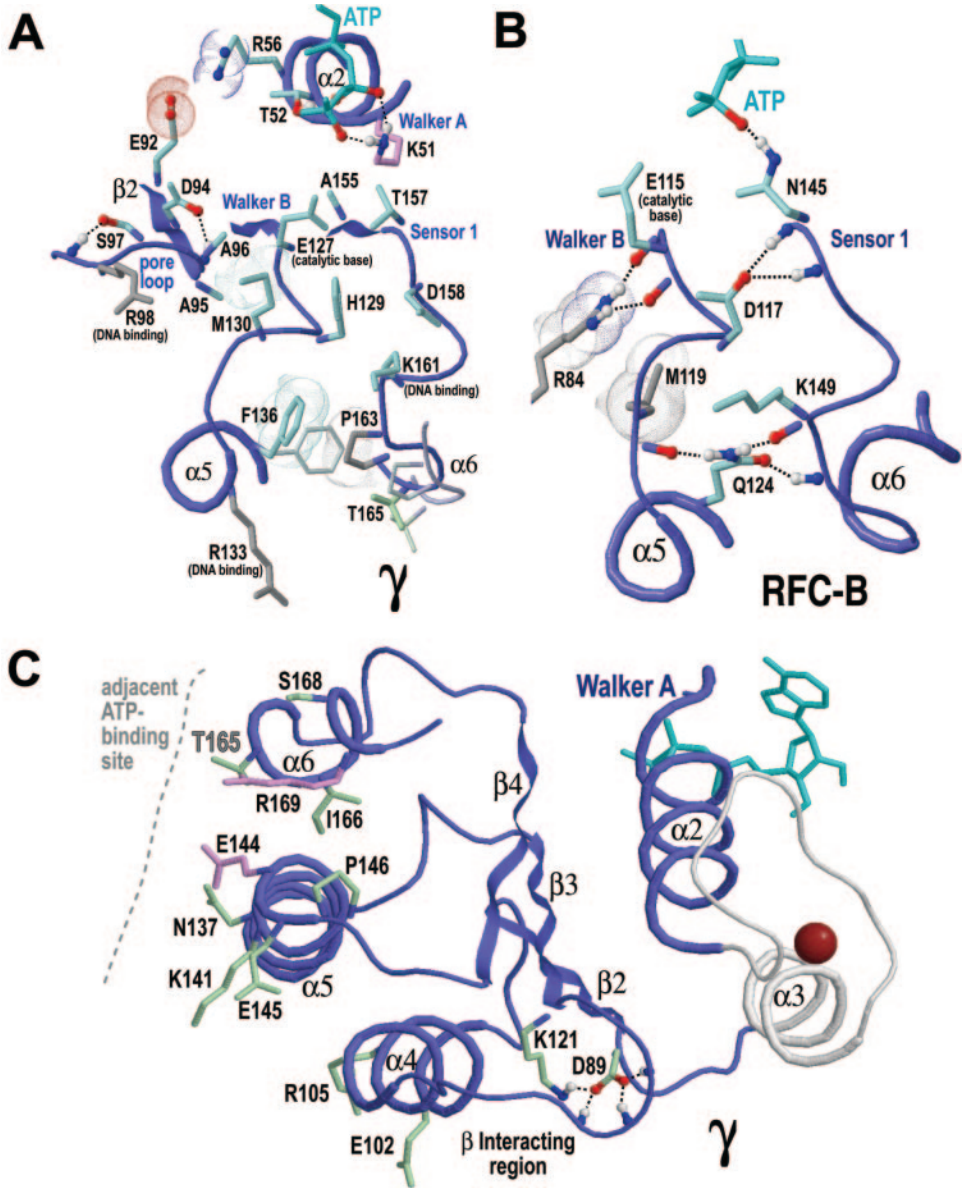

Figure 3. Conserved residues subject to constraints either shared by or distinguishing between the γ and δ′ subunits. Oxygen, nitrogen and hydrogen atoms predicted to form hydrogen bonds are colored red, blue and white, respectively. Hydrogens were added to structural coordinates using Reduce (59). Ionic and van der Waals interactions are shown as dot clouds. (**A**) ATP-bound form of γ showing residues (light cyan side-chains) that distinguish γ from δ′ subunits. Two poorly conserved arginines implicated in DNA binding ($R98^{\gamma}$ and $R133^{\gamma}$) are shown in gray. Within available crystal structures Phe136 exhibits two distinct conformational forms: one in which the plane of its aromatic ring is oriented perpendicular to the plane of a nearby proline (Pro163) side-chain ring (colored cyan and gray, respectively) (pdb code: 1NJFA) and another in which its aromatic ring is parallel to the proline ring (thin, light gray wireframe image) (pdb code: 1NJFB). The position of the proposed *trans*-acting catalytic threonine, Thr165, is also shown (colored light green) for these alternative forms. (**B**) Residues of RFC-B (pdb code: 1SXJ) corresponding either to several of the conserved residues in (A) (light cyan side-chains) or to an DNA-dependent ATPase activation mechanism (gray side-chains) proposed for RFC–clamp loaders (33). Note that main-chain oxygens on either side of the putative glutamate catalytic base ($E115^{RFC\text{-}B}$) (corresponding to $E127^{\gamma}$) form hydrogen bonds to a highly conserved arginine in RFC subunits ($R84^{RFC\text{-}B}$) postulated to inactivate ATPase activity. This arginine is very poorly conserved in bacterial γ subunits. Similarly, corresponding RFC ATPases conserve a glutamine ($Q124^{RFC\text{-}B}$) instead of Phe136γ, which is conserved in γ ATPases; this glutamine forms hydrogen bonds to loop regions preceding helices 5 and 6. (**C**) Conserved residues distinguishing γ and δ′ subunits from other AAA+ ATPases. Presumably because γ and δ′ both interact with an adjacent γ subunit, many of these residues (light green side-chains) tend to be located at this interface. Two highly conserved residues characteristic of all AAA+ ATPases (light magenta side-chains) also occur at this interface, namely the AAA+ arginine finger ($R169^{\gamma}$) and a glutamate ($E144^{\gamma}$) that can form a salt bridge with this arginine.

arginine appears to modulate DNA-dependent ATPase activity by undergoing a conformational change that moves it away from disruptively interacting with backbone oxygens on either side of the putative catalytic base ($Glu115^{RFC\text{-}B}$) and into contact with RNA-primed DNA thread through the center of the clamp (33). Given that γ subunits fail to conserve this arginine, bacterial clamp loaders presumably possess an alternative mechanism for DNA-dependent regulation of ATPase activity. This alternative mechanism could involve $His129^{\gamma}$.

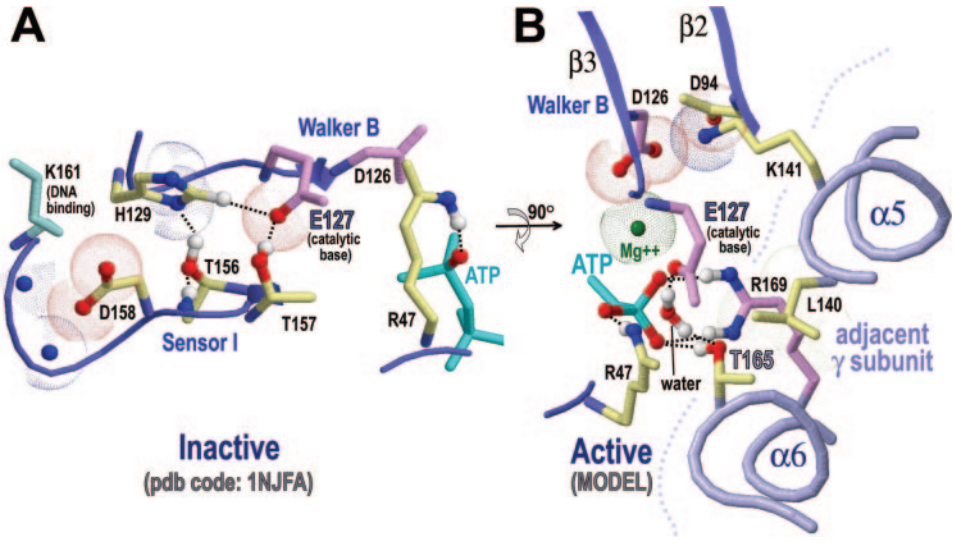

Figure 4. Conserved residues distinguishing γ from RFC ATPases and involved in the proposed activation mechanism. (**A**) Structural interactions corresponding to the proposed inactive form of γ ATPase. This form is predicted to inhibit ATP hydrolysis in the absence of RNA-primed DNA by drawing away the putative catalytic base (E127). For details see text. (**B**) Model of subunit-to-subunit interactions for the proposed active form of γ ATPase. A water molecule is activated for nucleophilic attack on γ-phosphate through interactions with the catalytic base (E127) and with the *trans*-acting threonine (T165). This model is based on RFC-A-to-RFC-B interactions within the RFC/ATP/clamp complex. Molecular modeling was performed using the KiNG program (http://kinemage.biochem.duke.edu/). For details see text.

Highly conserved histidines are often either associated with catalytic roles or serve as controllable elements in conformational changes (43). A possible function for $His129^{\gamma}$ is suggested by examining residues that, like His129 itself, distinguish γ from RFC subunits (Figure 2B) and that thus may play mechanistic roles unique to γ ATPases. Within available crystal structures several of these residues, namely $Thr156^{\gamma}$, $Thr157^{\gamma}$ and $Asp158^{\gamma}$, contact $His129^{\gamma}$ (Figure 4A) and often the side chain of $Thr156^{\gamma}$ is positioned to form a hydrogen bond with $His129^{\gamma}$ and with the backbone NH-group of $Asp158^{\gamma}$ (Figure 4A). These two hydrogen bonds link $His129^{\gamma}$ to the sensor 1 threonine ($Thr157^{\gamma}$) that is located between $Thr156^{\gamma}$ and $Asp158^{\gamma}$ and that also appears to form a hydrogen bond with the putative catalytic base, $Glu127^{\gamma}$. The side-chain oxygens of $Asp158^{\gamma}$ are positioned to electrostatically interact with the positive dipole moment created by the backbone of the loop connecting it to $Lys161^{\gamma}$, a residue implicated in DNA binding (26). (Unlike other basic residues of γ implicated in DNA binding, this lysine is also highly conserved in corresponding RFC ATPases.) Association of γ with DNA thus could influence the conformation, not only of $Lys161^{\gamma}$, but also of $Asp158^{\gamma}$, given the latter's proximity to $Lys161^{\gamma}$ and the fact that both γ and DNA backbone phosphates are negatively charged and thus mutually repel.

HYPOTHETICAL DNA-DEPENDENT REGULATORY MECHANISM INVOLVING His129

The interaction of $His129^{\gamma}$ with the putative catalytic base, $Glu127^{\gamma}$, and with these other residues and their proximity to $Lys161^{\gamma}$ suggests the following mechanism for DNA-dependent ATPase activation.

Inactive form

In the absence of DNA, inhibition of γ's ATPase activity could occur through protonation of one of $His129^{\gamma}$'s side-chain nitrogens (N_{δ}) via electron transfer beginning with the peptide bond between $Thr157^{\gamma}$ and $Asp158^{\gamma}$ and terminating in transfer of the side-chain –OH hydrogen of $Thr156^{\gamma}$ to $His129^{\gamma}$ (Figure 5, right to left panels). This process would result in full double-bond formation between the main-chain nitrogen of $Asp158^{\gamma}$ and the main-chain carbonyl carbon of $Thr157^{\gamma}$—one of two peptide bond resonance forms first proposed by Pauling *et al.* (44). The backbone oxygen of $Thr157^{\gamma}$ being solvent exposed might favor this resonance form by allowing the resultant negative charge on this oxygen to be stabilized by a solvent cation (Figure 5, left panel). As a result, $His129^{\gamma}$ would become positively charged to form a salt bridge with the negatively charged $Glu127^{\gamma}$. At the same time $Thr157^{\gamma}$ stabilizes the $His129^{\gamma}$–$Glu127^{\gamma}$ salt bridge interaction by forming a hydrogen bond with the side-chain oxygen of $Glu127^{\gamma}$ (Figures 4A and 5, left panel). The resultant redistribution of negative charge within the glutamate side chain and its repositioning prevents it from serving as a catalytic base for ATP hydrolysis.

Active form

Association of the γ clamp loader–ATP–clamp complex with RNA-primed DNA is likely to induce conformational changes in the loop containing $Asp158^{\gamma}$ and $Lys161^{\gamma}$. Because both of these residues interact with $His129^{\gamma}$, transient electrostatic interactions could favor electron transfer through the –OH group of $Thr156^{\gamma}$ to eliminate the positive charge on $His129^{\gamma}$ and to thereby disrupt the $His129^{\gamma}$–$Glu127^{\gamma}$ salt bridge (Figure 5, left to right). Upon release of $Glu127^{\gamma}$, its side-chain electron density could be

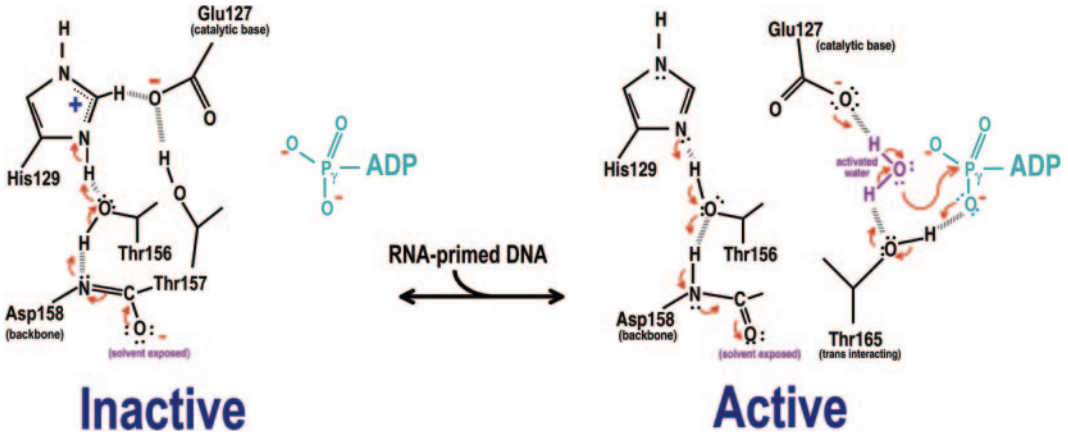

Figure 5. Proposed hypothetical clamp loader activation mechanism. Switching between inactive and active states occurs via an electron transfer chain involving His129 and residues in the Sensor 1 region (Thr156, Thr157 and Asp158). In the inactive form (left panel), this results in a positive charge on His129, which sequesters the catalytic base (Glu127) away from the γ-phosphate of bound ATP. In the active form (right panel), the charge on His129 is neutralized, which allows the catalytic base to hydrogen bond to and activate a water molecule for attack on the γ-phosphorous atom of ATP. The water molecule is activated through two proton extractions mediated by the side-chain oxygen of Glu127 and of a *trans*-interacting catalytic threonine (Thr165 in γ or Thr154 in δ′). For details see text.

redistributed—allowing it to serve as a catalytic base facilitating attack by an activated water molecule on the γ phosphate of ATP (Figure 5, right panel). (The hydrogen bonds formed by Thr156$^{\gamma}$ with the side-chain of His129$^{\gamma}$ and with the main-chain of Asp158$^{\gamma}$ might also be eliminated—though whether or not this occurs is unimportant to the proposed mechanism.)

POTENTIALLY FLEXIBLE REGIONS SURROUNDING His129

The nature of conserved residues distinguishing γ ATPase both from corresponding RFC ATPases and from inactive δ′ subunits (Figure 2B and D) supports the notion that γ's underlying mechanism requires that regions surrounding His129$^{\gamma}$ be conformationally flexible.

Conformational flexibility of Met130

Consider, for example, a conserved methionine (Met130$^{\gamma}$) that strikingly distinguishes γ ATPases from inactive δ′ subunits (Figure 2D). Methionine is conformationally flexible (43) inasmuch as it is the only unbranched hydrophobic amino acid and contains a side-chain sulphur atom, which provides some hydrogen-bonding capability. Thus buried regions required to undergo conformational changes might be more likely to conserve a methionine than other, less adaptable hydrophobic amino acids. Met130γ is sequence adjacent to and contacts His129$^{\gamma}$ [perhaps forming a non-bonded interaction with it (45)] and also contacts the putative catalytic base, Glu127$^{\gamma}$, as well as two alanines within a DAAS motif (position 94–97 in Figure 2B and D). The DAAS motif structurally corresponds to an NASD motif within RFC ATPases—the ATP- and ADP-bound forms of which exhibit distinct conformations (33). Moreover, the DAAS motif lies within the 'pore loop' of AAA+ ATPases: a region that provides most of the surface of the central pore (46), through which a number of AAA+ complexes thread their substrates (13). Hence, this pore region is likely to undergo conformational changes upon association with RNA-primed DNA. The short side-chains of the DAAS-motif alanines presumably are less restrictive than other amino acid residues and thus could allow the Met130$^{\gamma}$ side-chain greater conformational freedom.

Conformational flexibility of Phe136

A conserved phenylalanine (Phe136$^{\gamma}$) that distinguishes γ both from δ′ and from RFC ATPases (Figure 2D and B) and that is located directly below the main-chain of His129$^{\gamma}$ similarly manifests flexibility inasmuch as it occurs in two distinct conformational states (Figure 3A). Both of these conformations are observed within crystal structures of γ either bound or unbound to an ATP analog—suggesting that these alternative forms are not due to the mere presence or absence of ATP.

Within corresponding RFC ATPases this phenylalanine corresponds to a highly conserved glutamine (Q124$^{\text{RFC-B}}$). This glutamine forms characteristic hydrogen bonds (Figure 3B) that are well conserved within various RFC subunits and that structurally couple regions implicated in DNA-dependent activation with helices 5 and 6, which conserve residues interacting (*in trans*) with the ATP-binding site of an adjacent subunit (33). The existence of these hydrogen bonds is supported by all nine currently available crystal structure forms of eukaryotic and archaeal small RFC subunits, suggesting that this glutamine plays a critical structural role in proper positioning of these regions. It is thus rather surprising that this residue is replaced within γ ATPases by a conserved, conformationally flexible phenylalanine.

Phe136$^{\gamma}$, which is located in helix 5, establishes van der Waals contact with a proline (Pro163$^{\gamma}$) that is near the N-terminal end of helix 6 and that is conserved in ~70–80% of bacterial γ subunits. In one of γ's two conformational forms the plane of the phenylalanine aromatic ring is oriented perpendicular to the plane of Pro163's side-chain ring while in the other form it is parallel to the proline ring (Figure 3A). The distances between the α carbons of

Phe136$^{\gamma}$ and Pro163$^{\gamma}$ differ between these two forms by ~2.5 Å, indicating that the position of helix 5 relative to helix 6 within γ subunits significantly changes upon movement of this phenylalanine. This contrasts with the apparently rigid relative positioning of corresponding regions within RFC subunits due to the hydrogen bonds formed by the glutamine structurally corresponding to Phe136$^{\gamma}$ (i.e. Gln124$^{\text{RFC-B}}$ in Figure 3B). Moreover, the ATPase activity of an adjacent γ subunit seems likely to be modulated by Phe136$^{\gamma}$-associated conformational changes, inasmuch as these could reposition critical residues within helices 5 and 6 (Figure 3C) relative to the adjacent ATP-binding site.

ASSOCIATIONS WITH DNA-BINDING RESIDUES IN γ

Bacterial clamp loader γ ATPases might diverge from corresponding eukaryotic and archaeal RFC ATPases in these ways due to a fundamentally different mode of DNA-dependent activation. Indeed, basic residues in γ experimentally implicated in DNA binding (26), namely Arg98$^{\gamma}$, Lys100$^{\gamma}$, Arg133$^{\gamma}$ and Lys161$^{\gamma}$, are closely attached to regions harboring conserved residues that distinguish γ either from RFC ATPases, from δ′ or from both. Arg98$^{\gamma}$ and Lys100$^{\gamma}$ (both of which are poorly conserved) directly follow the DAAS motif (though only Arg98$^{\gamma}$ is shown in Figure 3A). Arg133$^{\gamma}$ (which likewise is only weakly conserved) is situated between His129$^{\gamma}$ and Phe136$^{\gamma}$ (Figure 3A). And Lys161$^{\gamma}$ (which is highly conserved in both γ and RFC ATPases) is within the loop connecting the Sensor 1 region (harboring residues 156–158) to helix 6 (harboring Thr165$^{\gamma}$, a putative *trans*-acting catalytic residue discussed at length below).

INTERACTIONS BETWEEN ADJACENT γ SUBUNITS

ATP hydrolysis by AAA+ ATPases is believed to require interaction with a *trans*-acting arginine finger donated by an adjacent AAA+ subunit and, in the case of γ ATPase, perhaps with additional *trans*-acting residues mediating either catalysis itself or proper subunit-to-subunit positioning upon binding of the complex to the clamp and to DNA. Such residues are likely subject to constraints distinguishing both γ and δ′ from other AAA+ proteins (Figure 2C) inasmuch as δ′ interacts with the adjacent γ_D subunit's ATP site in a manner similar to interaction of γ_D or γ_C with the adjacent γ subunit's ATP site (Figure 1A). As expected, most residues subject to these constraints occur at the subunit-to-subunit interface shared by γ and δ′ (Figure 3C), which corresponds to helices 4, 5 and 6.

Exploring what these constraints imply mechanistically is hindered somewhat in that currently available structures of the γ complex (11,19) correspond to inactive states and were determined in the absence of the clamp and of DNA. As a result, the interactions between critical residues observed in these structures might be mechanistically meaningless, and, indeed, the δ, γ_B, γ_C, γ_D and δ′ subunits within these complexes appear to be orientated rather haphazardly relative to each other. Thus, to help interpret these functional constraints, structural models of the ATP-bound form of the γ complex bound to the clamp were constructed based on structural analogy to related RFC subunits within the RFC–ATP–clamp complex (21). [The highly conserved arginine finger (Arg169$^{\gamma}$) and acidic residue (Glu144$^{\gamma}$) in helices 6 and 5, respectively, can help guide geometrically precise positioning of these helices relative to the adjacent ATP site.] In particular, because the interaction between the RFC-A and RFC-B subunits appears poised for action (21), these were used to model the interaction between γ subunits shown in Figure 4B.

A CRITICAL CATALYTIC ROLE FOR Thr165

By far the strongest constraint associated with interactions between adjacent γ subunits (Figure 2C) is imposed on a conserved threonine (Thr165$^{\gamma}$; Thr154$^{\delta'}$), which (based on modeling) can form a hydrogen bond with and thereby help properly position a water molecule for nucleophilic attack on the γ phosphate of ATP (Figures 4B and 5, right panel). Moreover, Thr165$^{\gamma}$ might also assist the catalytic base (Glu127$^{\gamma}$) by forming an –OH hydrogen bond with a γ-phosphate oxygen atom, thereby setting up an electron transfer network leading to the extraction of a proton from and thereby activating the nearby water molecule for nucleophilic attack (Figure 5, right panel). Incidentally, this arrangement ensures that catalysis occurs only after the interface with helices 5 and 6 of the adjacent γ or δ′ subunit is properly oriented, which presumably would only be true once the γ complex is bound to the clamp and to RNA-primed DNA.

Other residues subject to constraints distinguishing γ from corresponding RFC subunits (Figure 2B) might assist Thr165$^{\gamma}$ in this putative catalytic role. For example, within the available crystal structures of the γ subunit, Leu140$^{\gamma}$ packs against both Thr165$^{\gamma}$ and the AAA+ arginine finger (Arg169$^{\gamma}$) (Figure 4B), suggesting that its role is to properly position these residues for catalysis. Similarly, modeling of γ-to-γ subunit interactions indicates that Lys141$^{\gamma}$, which is next to Leu140$^{\gamma}$ in the sequence, is likely to interact electrostatically with two conserved acidic residues: one being the Walker B motif aspartate and another near the pore loop (Asp126$^{\gamma}$ and Asp94$^{\gamma}$ in Figure 4B, respectively). Within the RFC ATPases, the pore loop is characterized by an NxSD motif that manifests two distinct conformations proposed to correspond to active and inactive states (33). Although bacterial γ and δ′ subunits lack this NxSD motif, they conserve an alternative DxAS motif at the corresponding pore loop positions (Figure 2B and C). Electrostatic interactions involving Lys141$^{\gamma}$ might help couple positioning of the pore loop and the Walker B regions to the *trans*-acting catalytic residues (i.e. Arg169$^{\gamma}$ and Thr165$^{\gamma}$) and thus perhaps help couple sensing of cognate DNA to ATP hydrolysis.

ARG47 AS A SECOND, *CIS*-ACTING ARGININE FINGER

Thr165$^{\gamma}$ corresponds to a proline residue within the RFC-B subunit (Pro153$^{\text{RFC-B}}$). This proline contacts another proline (Pro355$^{\text{RFC-A}}$) within the adjacent RFC-A subunit—a residue corresponding to Arg47$^{\gamma}$. Arg47$^{\gamma}$ is specifically conserved within γ (Figure 2B and D) and is positioned to form a

hydrogen bond with the γ phosphate of ATP (Figure 4) and, in fact, does so in several of the available crystal structures.

Why does the γ subunit conserve an arginine ($Arg47^{\gamma}$) at a position corresponding to a conserved proline within RFC subunits? An answer is suggested by comparison with the RFC–clamp–ATP complex, for which an arginine ($Arg128^{RFC\text{-}B}$)—that is conserved in RFC subunits, but not in the corresponding γ and δ′ subunits—forms a hydrogen bond (*in trans*) to the γ phosphate of ATP bound to an adjacent subunit (21). Hence, RFC subunits donate two arginine fingers *in trans* to the adjacent ATP-binding site: the arginine finger that is generally shared by all AAA+ ATPases (e.g. $Arg157^{RFC\text{-}B}$ corresponding to $Arg169^{\gamma}$) and this additional arginine finger, which is conserved only in small RFC subunits (e.g. $Arg128^{RFC\text{-}B}$). However, within the γ complex this second *trans*-acting RFC-specific arginine finger appears to be functionally replaced by a *cis*-acting arginine unique to γ subunits, namely $Arg47^{\gamma}$—a change that may be required to complete the catalytic role of Thr165γ (or Thr154 in δ′), with which $Arg47^{\gamma}$ is predicted to interact. In particular, hydrogen bond formation between γ-phosphate oxygen atoms and Arg47γ (as well as with $Arg169^{\gamma}$) could help draw electrons away from the γ phosphorous atom (especially given arginine's positive charge) and thereby make it more susceptible to nucleophilic attack by an activated water molecule.

$Arg47^{\gamma}$ occupies the third position of the Walker A or P loop motif (Gx**R**xxGKT, where this position is bold and underlined), and several studies using vanadate as a transition state analog of phosphate indicate that in P loop NTPases the γ phosphate of ATP in the transition state is near the corresponding residue at this position. These include Ser180 in myosin (Gx**S**xxGKT) (47), Pro17 in adenylate kinase (Gx**P**xxGKgT) (48) and Ala158 in ATP synthase (Gx**A**xxGKT) (49). A more recent study (50) indicates that, in the transition state of ATP synthase, Mg^{2+} plays a key role in repositioning of the P loop to bring this third Walker A residue ($Ala158^{ATP\_synthase}$) into the catalytic pocket. This raises the possibility that $Arg47^{\gamma}$ undergoes a similar repositioning in the transition state of the γ subunit and thus further supports an important role for it in ATP hydrolysis and perhaps in nucleotide exchange. Incidentally, AAA+ modules within the Mg^{2+} chelatase BchI subunit (51) and within the BCS1 protein involved in biogenesis of mitochondrial respiratory chain complexes (52) also conserve an arginine at this third Walker A position.

CONCLUDING REMARKS

The similarities and differences in selective constraints imposed on various bacterial, eukaryotic and archaeal clamp loader subunits reflect similarities and differences in their underlying mechanisms. Examining these constraints in light of clamp loader structures can suggest feasible hypotheses regarding these mechanisms. Here this has led to the hypothesis that bacterial clamp loader ATPases are activated through DNA-dependent repositioning both of the catalytic base and of a *trans*-acting catalytic threonine donated by an adjacent γ or δ′ subunit. To test this hypothesis, mutagenesis experiments can be devised where a critical residue is replaced by the corresponding residue observed in related AAA+ ATPases or by an amino acid that—though unlikely to introduce structural perturbations—is inconsistent with the proposed mechanism. For example, mutating Thr165 to valine would merely replace its side-chain oxygen with a carbon and thereby would be predicted to eliminate catalysis without significantly perturbing other structural features of the γ complex. Similar substitutions might include R47P, H129D, M130L, F136Q, T156C, T156S and T157N. This and similar analyses of other AAA+ ATPases—such as RuvB, which likewise harbors a histidine and sensor 1 threonine capable of similar interactions with the putative catalytic base—should provide insight into the general mechanisms of the AAA+ class of molecular chaperones and into their functional divergence during evolution.

ACKNOWLEDGEMENTS

I thank Christian Speck for critical reading of the manuscript and helpful comments and Mike O'Donnell for helpful suggestions regarding an early version of this manuscript. This work was supported by NIH grant LM06747. Funding to pay the Open Access publication charges for this article was provided by this grant.

Conflict of interest statement. None declared.

REFERENCES

1. Waga,S. and Stillman,B. (1998) The DNA replication fork in eukaryotic cells. *Annu. Rev. Biochem.*, **67**, 721–751.
2. Jeruzalmi,D., O'Donnell,M. and Kuriyan,J. (2002) Clamp loaders and sliding clamps. *Curr. Opin. Struct. Biol.*, **12**, 217–224.
3. Stukenberg,P.T., Studwell-Vaughan,P.S. and O'Donnell,M. (1991) Mechanism of the sliding beta-clamp of DNA polymerase III holoenzyme. *J. Biol. Chem.*, **266**, 11328–11334.
4. Naktinis,V., Turner,J. and O'Donnell,M. (1996) A molecular switch in a replication machine defined by an internal competition for protein rings. *Cell*, **84**, 137–145.
5. Kong,X.P., Onrust,R., O'Donnell,M. and Kuriyan,J. (1992) Three-dimensional structure of the beta subunit of *E.coli* DNA polymerase III holoenzyme: a sliding DNA clamp. *Cell*, **69**, 425–437.
6. Yao,N., Turner,J., Kelman,Z., Stukenberg,P.T., Dean,F., Shechter,D., Pan,Z.Q., Hurwitz,J. and O'Donnell,M. (1996) Clamp loading, unloading and intrinsic stability of the PCNA, beta and gp45 sliding clamps of human, *E.coli* and T4 replicases. *Genes Cells*, **1**, 101–113.
7. Leu,F.P., Hingorani,M.M., Turner,J. and O'Donnell,M. (2000) The delta subunit of DNA polymerase III holoenzyme serves as a sliding clamp unloader in *Escherichia coli*. *J. Biol. Chem.*, **275**, 34609–34618.
8. Marians,K.J. (1992) Prokaryotic DNA replication. *Annu. Rev. Biochem.*, **61**, 673–719.
9. Bowman,G.D., Goedken,E.R., Kazmirski,S.L., O'Donnell,M. and Kuriyan,J. (2005) DNA polymerase clamp loaders and DNA recognition. *FEBS Lett.*, **579**, 863–867.
10. Onrust,R., Finkelstein,J., Turner,J., Naktinis,V. and O'Donnell,M. (1995) Assembly of a chromosomal replication machine: two DNA polymerases, a clamp loader, and sliding clamps in one holoenzyme particle III. Interface between two polymerases and the clamp loader. *J. Biol. Chem.*, **270**, 13366–13377.
11. Jeruzalmi,D., O'Donnell,M. and Kuriyan,J. (2001) Crystal structure of the processivity clamp loader gamma (gamma) complex of *E.coli* DNA polymerase III. *Cell*, **106**, 429–441.
12. Neuwald,A.F., Aravind,L., Spouge,J.L. and Koonin,E.V. (1999) AAA+: A class of chaperone-like ATPases associated with the assembly, operation, and disassembly of protein complexes. *Genome Res.*, **9**, 27–43.

13. Hanson,P.I. and Whiteheart,S.W. (2005) AAA+ proteins: have engine, will work. *Nature Rev. Mol. Cell. Biol.*, **6**, 519–529.
14. Walker,J.E., Saraste,M., Runswick,M.J. and Gay,N.J. (1982) Distantly related sequences in the alpha- and beta-subunits of ATP synthase, myosin, kinases and other ATP-requiring enzymes and a common nucleotide binding fold. *EMBO J.*, **1**, 945–951.
15. Studwell-Vaughan,P.S. and O'Donnell,M. (1991) Constitution of the twin polymerase of DNA polymerase III holoenzyme. *J. Biol. Chem.*, **266**, 19833–19841.
16. Majka,J. and Burgers,P.M. (2004) The PCNA-RFC families of DNA clamps and clamp loaders. *Prog. Nucleic Acid Res. Mol. Biol.*, **78**, 227–260.
17. Guenther,B., Onrust,R., Sali,A., O'Donnell,M. and Kuriyan,J. (1997) Crystal structure of the δ′ subunit of the clamp-loader complex of *E.coli* DNA polymerase III. *Cell*, **91**, 335–345.
18. Podobnik,M., Weitze,T.F., O'Donnell,M. and Kuriyan,J. (2003) Nucleotide-Induced conformational changes in an isolated *Escherichia coli* DNA polymerase III clamp loader subunit. *Structure (Camb.)*, **11**, 253–263.
19. Kazmirski,S.L., Podobnik,M., Weitze,T.F., O'Donnell,M. and Kuriyan,J. (2004) Structural analysis of the inactive state of the *Escherichia coli* DNA polymerase clamp-loader complex. *Proc. Natl Acad. Sci. USA*, **101**, 16750–16755.
20. Jeruzalmi,D., Yurieva,O., Zhao,Y., Young,M., Stewart,J., Hingorani,M., O'Donnell,M. and Kuriyan,J. (2001) Mechanism of processivity clamp opening by the delta subunit wrench of the clamp loader complex of *E.coli* DNA polymerase III. *Cell*, **106**, 417–428.
21. Bowman,G.D., O'Donnell,M. and Kuriyan,J. (2004) Structural analysis of a eukaryotic sliding DNA clamp–clamp loader complex. *Nature*, **429**, 724–730.
22. Oyama,T., Ishino,Y., Cann,I.K., Ishino,S. and Morikawa,K. (2001) Atomic structure of the clamp loader small subunit from *Pyrococcus furiosus*. *Mol. Cell*, **8**, 455–463.
23. Stewart,J., Hingorani,M.M., Kelman,Z. and O'Donnell,M. (2001) Mechanism of beta clamp opening by the delta subunit of *Escherichia coli* DNA polymerase III holoenzyme. *J. Biol. Chem.*, **276**, 19182–19189.
24. Bloom,L.B., Turner,J., Kelman,Z., Beechem,J.M., O'Donnell,M. and Goodman,M.F. (1996) Dynamics of loading the beta sliding clamp of DNA polymerase III onto DNA. *J. Biol. Chem.*, **271**, 30699–30708.
25. Ason,B., Bertram,J.G., Hingorani,M.M., Beechem,J.M., O'Donnell,M., Goodman,M.F. and Bloom,L.B. (2000) A model for *Escherichia coli* DNA polymerase III holoenzyme assembly at primer/template ends DNA triggers a change in binding specificity of the gamma complex clamp loader. *J. Biol. Chem.*, **275**, 3006–3015.
26. Goedken,E.R., Kazmirski,S.L., Bowman,G.D., O'Donnell,M. and Kuriyan,J. (2005) Mapping the interaction of DNA with the *Escherichia coli* DNA polymerase clamp loader complex. *Nature Struct. Mol. Biol.*, **12**, 183–190.
27. Ason,B., Handayani,R., Williams,C.R., Bertram,J.G., Hingorani,M.M., O'Donnell,M., Goodman,M.F. and Bloom,L.B. (2003) Mechanism of loading the *Escherichia coli* DNA polymerase III beta sliding clamp on DNA. Bona fide primer/templates preferentially trigger the gamma complex to hydrolyze ATP and load the clamp. *J. Biol. Chem.*, **278**, 10033–10040.
28. O'Donnell,M., Jeruzalmi,D. and Kuriyan,J. (2001) Clamp loader structure predicts the architecture of DNA polymerase III holoenzyme and RFC. *Curr. Biol.*, **11**, R935–946.
29. Davey,M.J., Jeruzalmi,D., Kuriyan,J. and O'Donnell,M. (2002) Motors and switches: AAA+ machines within the replisome. *Nature Rev. Mol. Cell Biol.*, **3**, 826–835.
30. Neuwald,A.F. and Liu,J.S. (2004) Gapped alignment of protein sequence motifs through Monte Carlo optimization of a hidden Markov model. *BMC Bioinformatics*, **5**, 157.
31. Neuwald,A.F., Kannan,N., Poleksic,A., Hata,N. and Liu,J.S. (2003) Ran's C-terminal, basic patch and nucleotide exchange mechanisms in light of a canonical structure for Rab, Rho, Ras and Ran GTPases. *Genome Res.*, **13**, 673–692.
32. Neuwald,A.F. (2006) Bayesian shadows of molecular mechanisms cast in the light of evolution. *Trends Biochem. Sci.*, **31**, 374–382.
33. Neuwald,A.F. (2005) Evolutionary clues to eukaryotic DNA clamp-loading mechanisms: analysis of the functional constraints imposed on replication factor C AAA+ ATPases. *Nucleic Acids Res.*, **33**, 3614–3628.
34. Saraste,M., Sibbald,P.R. and Wittinghofer,A. (1990) The P-loop—a common motif in ATP- and GTP-binding proteins. *Trends Biochem. Sci.*, **15**, 430–434.
35. Koonin,E.V. (1993) A common set of conserved motifs in a vast variety of putative nucleic acid-dependent ATPases including MCM proteins involved in the initiation of eukaryotic DNA replication. *Nucleic Acids Res.*, **21**, 2541–2547.
36. Lenzen,C.U., Steinmann,D., Whiteheart,S.W. and Weis,W.I. (1998) Crystal structure of the hexamerization domain of N-ethylmaleimide-sensitive fusion protein. *Cell*, **94**, 525–536.
37. Yu,R.C., Hanson,P.I., Jahn,R. and Brunger,A.T. (1998) Structure of the ATP-dependent oligomerization domain of N-ethylmaleimide sensitive factor complexed with ATP. *Nature Struct. Biol.*, **5**, 803–811.
38. Hattendorf,D.A. and Lindquist,S.L. (2002) Cooperative kinetics of both Hsp104 ATPase domains and interdomain communication revealed by AAA sensor-1 mutants. *EMBO J.*, **21**, 12–21.
39. Ahmadian,M.R., Stege,P., Scheffzek,K. and Wittinghofer,A. (1997) Confirmation of the arginine-finger hypothesis for the GAP-stimulated GTP-hydrolysis reaction of Ras. *Nature Struct. Biol.*, **4**, 686–689.
40. Johnson,A. and O'Donnell,M. (2003) Ordered ATP hydrolysis in the gamma complex clamp loader AAA+ machine. *J. Biol. Chem.*, **278**, 14406–14413.
41. Snyder,A.K., Williams,C.R., Johnson,A., O'Donnell,M. and Bloom,L.B. (2004) Mechanism of loading the *Escherichia coli* DNA polymerase III sliding clamp: II. Uncoupling the beta and DNA binding activities of the gamma complex. *J. Biol. Chem.*, **279**, 4386–4393.
42. Orelle,C., Dalmas,O., Gros,P., Di Pietro,A. and Jault,J.M. (2003) The conserved glutamate residue adjacent to the Walker-B motif is the catalytic base for ATP hydrolysis in the ATP-binding cassette transporter BmrA. *J. Biol. Chem.*, **278**, 47002–47008.
43. Richardson,D.C.R. and Richardson,J.S. (1989) In Fasman,G.D. (ed.), *Prediction of Protein Structure and The Principles of Protein Conformation*. Plenum, NY, pp. 1–98.
44. Pauling,L., Corey,R.B. and Branson,H.R. (1951) The structure of proteins; two hydrogen-bonded helical configurations of the polypeptide chain. *Proc. Natl Acad. Sci. USA*, **37**, 205–211.
45. Pal,D. and Chakrabarti,P. (2001) Non-hydrogen bond interactions involving the methionine sulfur atom. *J. Biomol. Struct. Dyn.*, **19**, 115–128.
46. Wang,J., Song,J.J., Franklin,M.C., Kamtekar,S., Im,Y.J., Rho,S.H., Seong,I.S., Lee,C.S., Chung,C.H. and Eom,S.H. (2001) Crystal structures of the HslVU peptidase–ATPase complex reveal an ATP-dependent proteolysis mechanism. *Structure*, **9**, 177–184.
47. Cremo,C.R., Grammer,J.C. and Yount,R.G. (1989) Direct chemical evidence that serine 180 in the glycine-rich loop of myosin binds to ATP. *J. Biol. Chem.*, **264**, 6608–6611.
48. Cremo,C.R., Loo,J.A., Edmonds,C.G. and Hatlelid,K.M. (1992) Vanadate catalyzes photocleavage of adenylate kinase at proline-17 in the phosphate-binding loop. *Biochemistry*, **31**, 491–497.
49. Ko,Y.H., Bianchet,M., Amzel,L.M. and Pedersen,P.L. (1997) Novel insights into the chemical mechanism of ATP synthase. Evidence that in the transition state the gamma-phosphate of ATP is near the conserved alanine within the P-loop of the beta-subunit. *J. Biol. Chem.*, **272**, 18875–18881.
50. Ko,Y.H., Hong,S. and Pedersen,P.L. (1999) Chemical mechanism of ATP synthase. Magnesium plays a pivotal role in formation of the transition state where ATP is synthesized from ADP and inorganic phosphate. *J. Biol. Chem.*, **274**, 28853–28856.
51. Armstrong,G.A., Alberti,M., Leach,F. and Hearst,J.E. (1989) Nucleotide sequence, organization, and nature of the protein products of the carotenoid biosynthesis gene cluster of *Rhodobacter capsulatus*. *Mol. Gen. Genet.*, **216**, 254–268.
52. Petruzzella,V., Tiranti,V., Fernandez,P., Ianna,P., Carrozzo,R. and Zeviani,M. (1998) Identification and characterization of human cDNAs specific to BCS1, PET112, SCO1, COX15, and COX11, five genes involved in the formation and function of the mitochondrial respiratory chain. *Genomics*, **54**, 494–504.
53. Johnson,A. and O'Donnell,M. (2005) Cellular DNA replicases: components and dynamics at the replication fork. *Annu. Rev. Biochem.*, **74**, 283–315.

54. O'Donnell,M. and Kuriyan,J. (2006) Clamp loaders and replication initiation. *Curr. Opin. Struct. Biol.*, **16**, 35–41.
55. Sayle,R.A. and Milner-White,E.J. (1995) RASMOL: biomolecular graphics for all. *Trends Biochem. Sci.*, **20**, 374.
56. Altschul,S.F., Madden,T.L., Schaffer,A.A., Zhang,J., Zhang,Z., Miller,W. and Lipman,D.J. (1997) Gapped BLAST and PSI-BLAST: a new generation of protein database search programs. *Nucleic Acids Res.*, **25**, 3389–3402.
57. Shindyalov,I.N. and Bourne,P.E. (1998) Protein structure alignment by incremental combinatorial extension (CE) of the optimal path. *Protein Eng.*, **11**, 739–747.
58. Neuwald,A.F. (2003) Evolutionary clues to DNA polymerase III beta clamp structural mechanisms. *Nucleic Acids Res.*, **31**, 4503–4516.
59. Word,J.M., Lovell,S.C., LaBean,T.H., Taylor,H.C., Zalis,M.E., Presley,B.K., Richardson,J.S. and Richardson,D.C. (1999) Visualizing and quantifying molecular goodness-of-fit: small-probe contact dots with explicit hydrogen atoms. *J. Mol. Biol.*, **285**, 1711–1733.